

tions determine the three polarizabilities characterizing the $4p$ level. These are tabulated in Table I along with the predictions of the Bates and Daamgard theory. The agreement is seen to be good.

An interesting point arises from the fact that in the limit of zero-orbit coupling it can be shown² that

$$\alpha(4^2p_{\frac{1}{2}} \pm \frac{1}{2}) = \frac{1}{2}[\alpha(4^2p_{\frac{3}{2}} \pm \frac{3}{2}) + \alpha(4^2p_{\frac{3}{2}} \pm \frac{1}{2})].$$

This relationship is seen to be very well satisfied by the actual measurements, in contradistinction to the case of the first excited p state in cesium, which shows marked spin-orbit effects.

*Work supported by the U. S. Atomic Energy Commission.

¹D. R. Bates and A. Daamgard, *Phil. Trans. Roy. Soc. London* **A242**, 101 (1949).

²R. Marrus, D. McColm, and J. Yellin, *Phys. Rev.* **147**, 55 (1966).

³R. Marrus and D. McColm, *Phys. Rev. Letters* **15**, 813 (1965).

⁴R. Marrus, E. Wang, and J. Yellin, *Phys. Rev. Letters* **19**, 1 (1967).

⁵P. Buck and I. I. Rabi, *Phys. Rev.* **107**, 1291 (1957); R. W. Schmieder, A. Lurio, and W. Happer, *Phys. Rev.* **173**, 76 (1968).

⁶A. Salop, E. Pollack, and B. Bederson, *Phys. Rev.* **124**, 1431 (1961).

ESR Spectrum and Structure of HCN^- in KCl at 4°K *

Frank J. Adrian, Edward L. Cochran, Vernon A. Bowers, and Barry C. Weatherley[†]

Applied Physics Laboratory, The Johns Hopkins University, Silver Spring, Maryland

(Received 22 July 1968)

A previous electron-spin resonance (ESR) study of HCN^- in KCl at 77°K yielded an isotropic spectrum indicating rapid tumbling of the radical. At 4.2°K this tumbling is frozen out and ESR spectra recorded at this temperature are anisotropic, permitting a complete determination of the magnetic parameters of HCN^- . The experimental results show that the planar radicals lie in $\{110\}$ crystal planes with the CN bonds parallel to $\langle 110 \rangle$ crystal axes. The components of the electronic g -factor tensor, the proton hyperfine-splitting (hfs) tensor, and nitrogen hfs tensor are as follows: $g_1 = 2.0023$, $g_2 = 2.0005$, and $g_3 = 2.0035$; $A_1^{(\text{H})} = 136.5$, $A_2^{(\text{H})} = 141.3$, and $A_3^{(\text{H})} = 131.3$ Oe; and $A_1^{(\text{N})} = 20.9$ and $A_2^{(\text{N})} = A_3^{(\text{N})} = 0.0$ Oe. Axis 1 lies in the molecular plane and is perpendicular to the CN bond, axis 2 is parallel to the CN bond, and axis 3 is perpendicular to the molecular plane. The carbon-13 hfs tensor has the components: $A_1^{(\text{C})} = 90.0$, $A_2^{(\text{C})} = 65.6$, and $A_3^{(\text{C})} = 68.6$ Oe, where axes 1' and 2' lie in the molecular plane and make angles of 34° with axes 1 and 2, respectively. From these results we deduce an approximate value of 131° for the HCN bond angle and the following values for the unpaired electron density on the hydrogen, nitrogen, and carbon atoms: $\rho_{\text{H}} = 0.27$, $\rho_{\text{C}} = 0.32$ and $\rho_{\text{N}} = 0.41$.

INTRODUCTION

Electron-spin resonance (ESR) studies have shown that ultraviolet or gamma irradiation of cyanide-doped alkali halide crystals at 77°K followed by warming briefly to around 280°K and recoiling to 77°K produces the HCN^- radical ion.¹⁻³ The initial step in this process is apparently the photolytic dissociation of hydroxide ions, present as an impurity in the alkali halide, to give hydrogen atoms which at 77°K are trapped interstitially in the crystal. Warming the crystal

permits the H atoms to diffuse about and react with CN^- ions to form HCN^- ions.

At 77°K the ESR spectrum of HCN^- is isotropic indicating that the radical is rotating or reorienting rapidly enough to average out any anisotropies which may be present in its magnetic Hamiltonian.¹⁻³ We now report the ESR spectra of this center in KCl crystals at 4°K at which temperature the spectra are anisotropic indicating that the tumbling of the radicals has been frozen out. These measurements permit a complete determination of the magnetic parameters and of the orientation of HCN^- in the KCl crystal.⁴

EXPERIMENTAL

Cyanide-doped KCl crystals were drawn under nitrogen from a 95% KCl, 5% KCN melt contained in a platinum crucible. Failure to rigorously exclude oxygen from contact with the molten salt resulted in the formation of gas bubbles within the melt, indicating the occurrence of some chemical degradation. Crystals grown from such melts gave generally complex ESR spectra whereas in oxygen-free systems only HCN^- was observed.

Paramagnetic centers were generated in the doped crystals by photolysis at 77°K with a 100-W medium-pressure mercury arc in a quartz envelope, followed by rapid warming to 280°K and recooling. ESR measurements were made at X band in a TE011 circular cavity. The sample was contained in the quartz finger of a dewar containing liquid helium which extended into the cavity. This dewar and the cavity were immersed in a Styrofoam container filled with liquid nitrogen. The orientation dependence of the spectrum was studied by rotating the sample about the $\langle 100 \rangle$ crystal axis perpendicular to the external magnetic field.

RESULTS AND DISCUSSION

The magnetic interactions of HCN^- are described by the Hamiltonian⁵

$$\mathcal{H} = \beta \vec{H} \cdot \vec{g} \cdot \vec{S} + \vec{S} \cdot \vec{A} \cdot \vec{I}^{(H)} + \vec{S} \cdot \vec{A} \cdot \vec{I}^{(N)} + \vec{S} \cdot \vec{A} \cdot \vec{I}^{(C)} \quad (1)$$

Here, \vec{H} is the external magnetic field, β is the Bohr magneton, \vec{S} is the electron spin, and \vec{g} is the electronic g -factor tensor. The spins of the hydrogen, nitrogen and carbon nuclei are denoted as $\vec{I}^{(H)}$, $\vec{I}^{(N)}$, and $\vec{I}^{(C)}$, respectively, and $\vec{A}^{(H)}$, $\vec{A}^{(N)}$, and $\vec{A}^{(C)}$ are the corresponding hyperfine-splitting (hfs) tensors. The nuclear Zeeman terms have been omitted from the foregoing Hamiltonian. Neglect of these terms can be justified *a posteriori* from our results which will show that the proton and carbon hfs splittings are always large compared to the Zeeman interactions of these nuclei, while the nitrogen Zeeman splitting is small compared to the width of the lines in the ESR spectrum.

The anisotropic ESR spectrum of an unsymmetrical molecule such as HCN^- , which contains several magnetic nuclei, can be quite complicated. Fortunately, the ESR spectrum of HCN^- at 4°K is relatively simple when the magnetic field is oriented either along the $[100]$ or the $[110]$ crystal axes, and these spectra are sufficient to determine the magnetic constants of the molecule and its orientation in the KCl crystal. It is also helpful to treat first the spectrum of the abundant isotopic species H^{12}CN^- to obtain \vec{g} , $\vec{A}^{(H)}$, and $\vec{A}^{(N)}$. This facilitates the analysis of the spectrum of samples enriched in carbon-13 to obtain $\vec{A}^{(C)}$.

 H^{12}CN^-

The ESR spectra of H^{12}CN^- at 4°K for the magnetic field oriented along the $[100]$ and $[110]$ cry-

stal axes are shown in Figs. 1 and 2, respectively. The spectrum for H^{12}CN^- is especially simple. It consists of a pair of triplets in which the doublet splitting is 136.5 Oe and the triplet splitting is 20.9 Oe. The triplet splitting is due to the nitrogen hfs and the triplet intensity ratio of (1:5:5:1) can be accounted for only if the nitrogen hfs of any HCN^- molecule is 20.9 Oe along one of the $\langle 100 \rangle$ crystal axes and zero along the other two $\langle 100 \rangle$ axes. [The theoretical intensity ratio for this assignment is (1:7:1) which is in satisfactory agreement with the observed intensity ratio when one considers that anything less than exact coincidence of the individual lines which comprise the strong center lines of the triplets will broaden this line slightly and reduce its intensity.] These results for the nitrogen hfs are especially useful in the analysis of the HCN^- spectrum because it is readily shown from Eq. (1) that a vanishing hyperfine splitting can occur only if one or more of the principal components of the hfs tensor has the value zero. Thus it follows immediately that $\vec{A}^{(N)}$ is axially symmetric with $A_{\parallel}^{(N)} = 20.9$ and $A_{\perp}^{(N)} = 0.0$ Oe, and that for any given HCN^- molecule, the symmetry axis of $\vec{A}^{(N)}$ is along a $[100]$ crystal axis.

The fact that the doublet splitting is the same for all the lines requires that the components of $\vec{A}^{(H)}$ along the three $\langle 100 \rangle$ axes have the same value, namely, 136.5 Oe. This quantity must be equal to the isotropic proton hfs constant ($A_0^{(H)}$) which has a measured value of 137.5 Oe at 77°K.¹

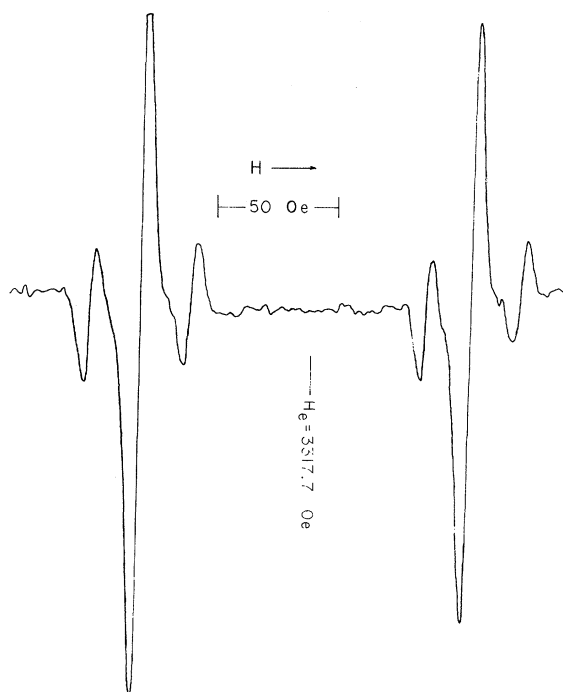


FIG. 1. ESR spectrum of H^{12}CN^- in KCl at 4°K for the magnetic field parallel to a $[100]$ crystal axis. In this and subsequent figures, H_e denotes the magnetic-field strength for resonance of the free electron.

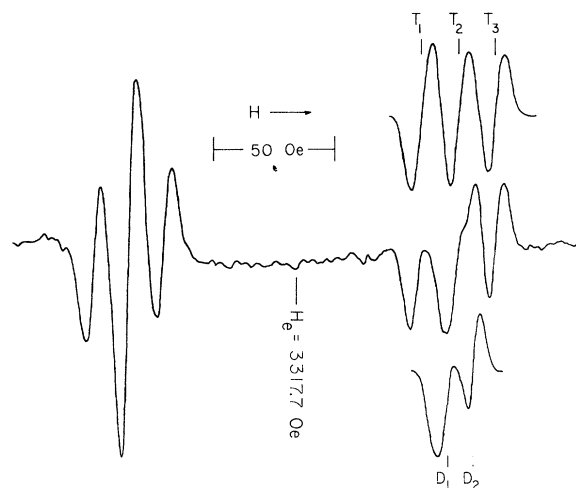


FIG. 2. ESR spectrum of H^{12}CN^- in KCl at 4°K for the magnetic field parallel to a $\langle 110 \rangle$ crystal axis.

The agreement between these quantities is satisfactory in view of the fact that hfs interaction constants are often slightly temperature dependent. The fact that all the splittings in this spectrum can be accounted for by the proton and nitrogen hfs requires that the components of \vec{g} along the three $\langle 100 \rangle$ crystal axes all have the same value. The common value of these components of g is 2.0023 which is in good agreement with the value of 2.0022 found for the isotropic g factor at 77°K .¹

The spectrum for $\text{H} \parallel [110]$, Fig. 2, is also relatively simple. The low-field portion is a simple triplet with a splitting of 14.8 Oe and an intensity ratio of (2:5:2). The high-field portion of this spectrum is more complex consisting of a broad complex center line and two outer lines with the same splitting and nearly the same shape and intensity as the outer lines of the low-field triplet. Using the knowledge that the triplet splitting is due to the nitrogen hfs, it is possible to decompose the high-field portion of the spectrum into a triplet and a doublet. The lines which make up the high-field portion of the spectrum are shown separately in Fig. 2 where, for later reference, the doublet lines are denoted as D_1 and D_2 while the triplet lines are denoted as T_1 , T_2 , and T_3 .

The 14.8-Oe nitrogen hfs triplet is due to those molecules which are oriented so that the magnetic field makes a 45° angle with the $[100]$ crystal axis which is the symmetry axis of their nitrogen hfs tensor. Two thirds of the HCN^- molecules will be oriented in this way assuming that the molecules are randomly distributed among all the orientations which they may assume in the KCl crystal. The remaining HCN^- molecules will be oriented so that the magnetic field is perpendicular to the symmetry axis of $\vec{A}^{(\text{N})}$, giving a nitrogen hfs of zero. This will lead to the intensity ratio of (2:5:2) observed for the low-field triplet provided that the values of the components of $\vec{A}^{(\text{H})}$ and \vec{g} are such that the center line of the 14.8-Oe

triplet and the lines with zero nitrogen hfs coincide exactly. This coincidence does not occur, however, in the high portion of the spectrum, where anisotropies in $\vec{A}^{(\text{H})}$ and \vec{g} split the lines for which $A^{(\text{N})} = 0$ into the doublet D_1 and D_2 .

These results provide enough data to determine all the components of \vec{g} and $\vec{A}^{(\text{H})}$. Table I gives the components of \vec{g} , $\vec{A}^{(\text{H})}$, and $\vec{A}^{(\text{N})}$ in an axis system composed of one of the $\langle 100 \rangle$ crystal axes and the two $\langle 110 \rangle$ axes which are perpendicular to this axis. These axes are denoted as \vec{j}_1 , \vec{j}_2 , \vec{j}_3 , respectively, and are illustrated in Fig. 3. Thus our results refer to an HCN^- radical which is oriented so that \vec{j}_1 is the symmetry axis of its nitrogen hfs tensor. All the components of $\vec{A}^{(\text{H})}$ and $\vec{A}^{(\text{N})}$ must have the same sign if they are to be consistent with the observed isotropic proton and nitrogen hfs constants. Theoretical considerations which will be discussed later suggest that the sign of these quantities is positive.

As discussed previously, the values of the components of $\vec{A}^{(\text{N})}$ and of the quantities g_1 and $A_1^{(\text{H})}$ were determined from the $\text{H} \parallel [100]$ spectrum. The values of g_2 , g_3 , $A_2^{(\text{H})}$ and $A_3^{(\text{H})}$ were determined from the $\text{H} \parallel [110]$ spectrum (Fig. 2). The specific lines used in this determination were the center line of the low-field triplet and the doublet lines D_1 and D_2 , that is, those lines for which $A^{(\text{N})} = 0$ indicating that the magnetic field was along a $\langle 110 \rangle$ axis which was perpendicular to the symmetry axis of $\vec{A}^{(\text{N})}$.

The measured values of the electronic g factors and the proton hfs constants of the remaining lines of the $\text{H} \parallel [110]$ spectrum, namely, those lines for which $A^{(\text{N})} = 14.8$ Oe indicating that the magnetic field makes a 45° angle with the symmetry axis of $\vec{A}^{(\text{N})}$, show that the axes \vec{j}_1 , \vec{j}_2 , and \vec{j}_3 , are the principal axes of both \vec{g} and $\vec{A}^{(\text{H})}$. [It has already been shown from the $\text{H} \parallel \langle 100 \rangle$ spectrum that these are the principal axes of $\vec{A}^{(\text{N})}$.] The reason for this is that all these lines have the same g factor (2.0020) and proton hyperfine splitting (136.1 Oe). This would not be the case if either \vec{g} or $\vec{A}^{(\text{H})}$ had off-diagonal components in this axis system. Also, using the results given in Table I, a computation of the electronic g factor and proton hyperfine splitting along those $\langle 110 \rangle$ crystal axes which make a 45° angle with \vec{j}_1 , gives 2.0022 for g and 136.4 Oe for $A^{(\text{H})}$ in excellent agreement with the experimental results. Finally, the results given in Table I predict that the electronic g factor and proton hyperfine splitting along the $\langle 100 \rangle$ crystal axes perpendicular to \vec{j}_1 will be 2.0020 and 136.7 Oe, in good agreement with the observation that the components of \vec{g} have the common value of 2.0023 along all three $\langle 100 \rangle$ axes while the com-

TABLE I. Principal components of the electronic g -factor tensor and the proton and nitrogen hyperfine splitting tensors of HCN^- . Components of the hyperfine splitting tensors are in oersteds.

$g_1 = 2.0023$	$A_1^{(\text{H})} = 136.5$	$A_1^{(\text{N})} = 20.9$
$g_2 = 2.0005$	$A_2^{(\text{H})} = 141.3$	$A_2^{(\text{N})} = 0.0$
$g_3 = 2.0035$	$A_3^{(\text{H})} = 131.3$	$A_3^{(\text{N})} = 0.0$

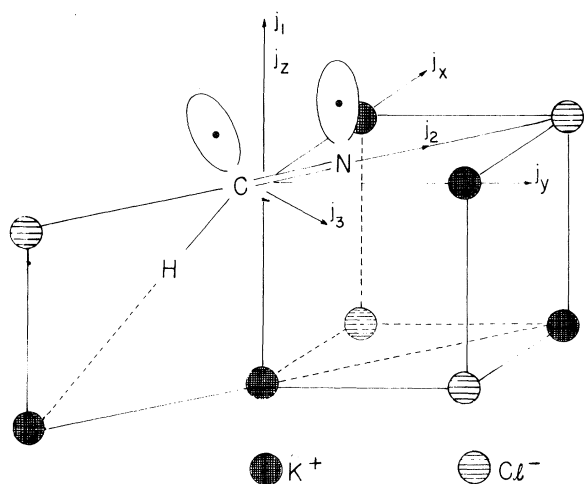


FIG. 3. Orientation of the HCN^- radical anion in the KCl crystal.

ponents of $\vec{A}(\text{H})$ along these three axes have a common value of 136.5 Oe.

These results together with a few elementary theoretical considerations are sufficient to determine the orientation of HCN^- in the KCl crystal. The observation that $\vec{A}(\text{N})$ is axially symmetric together with the fact that HCN^- , like the formyl radical (HCO),⁶ is a σ electron radical strongly suggests that the unpaired electron density on the nitrogen atom is located in that in-plane nitrogen $2p$ orbital which is perpendicular to the CN bond. This orbital will be the symmetry axis of $\vec{A}(\text{N})$ and, therefore, is oriented along the $[100]$ crystal axis which is denoted as \vec{j}_1 in Fig. 3. Moreover, the axis perpendicular to the molecular plane must be a symmetry axis of all the magnetic tensors of HCN^- and it has been shown that the remaining principal axes of these tensors are the $\langle 110 \rangle$ crystal axes perpendicular to the symmetry axis of $\vec{A}(\text{N})$. Therefore one of the $\langle 110 \rangle$ crystal axes must be perpendicular to the molecular plane of any HCN^- molecule so our complete picture of the orientation of these radicals, as shown in Fig. 3, is that they lie in $\{110\}$ crystal planes with the CN bonds parallel to $\langle 110 \rangle$ crystal axes. Theoretical considerations about g factor shifts in molecules of this type,⁶ which are supported by the experimental results on HCO ,⁶ indicate that the positive g -factor shift is associated with the axis perpendicular to the molecular plane, while the negative g -factor shift corresponds to an axis in the approximate direction of the CN bond. Thus we take \vec{j}_2 to be parallel to the CN bond and \vec{j}_3 to be perpendicular to the molecular plane.

H^{13}CN^-

The ESR spectra at 4°K of HCN^- enriched to 50% in carbon 13 are shown for the magnetic field parallel to the $[100]$ and $[110]$ crystal axes in Figs. 4 and 5, respectively. One puzzling

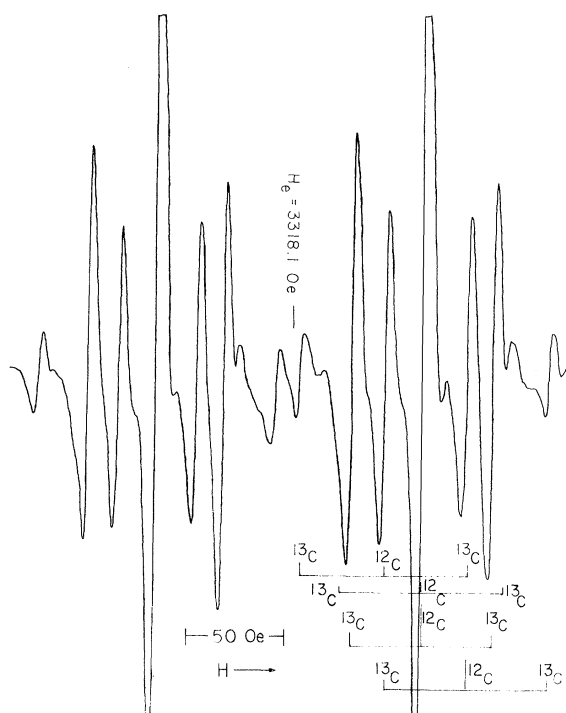


FIG. 4. ESR spectrum of 50% H^{12}CN^- and 50% H^{13}CN^- in KCl at 4°K for the magnetic field parallel to a $[100]$ crystal axis.

feature of these spectra is that the intensity of the H^{13}CN^- lines is considerably less than the expected value of one half the intensity of the corresponding H^{12}CN^- lines, whereas the isotropic spectrum observed at 77°K shows the expected intensity ratio. We have no explanation of this phenomenon beyond the possibility that the lines, which are known to have a long relaxation

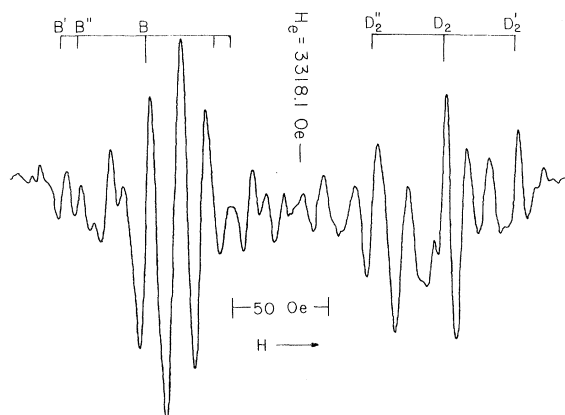


FIG. 5. ESR spectrum of 50% H^{12}CN^- and 50% H^{13}CN^- in KCl at 4°K for the magnetic field parallel to a $[110]$ crystal axis.

time at 4°K, are slightly saturated and that the H¹³CN⁻ lines are somewhat more saturated than are the H¹²CN⁻ lines. In any event, this effect is not likely to alter the positions of the lines and we will not consider it further.

The spectrum for H||[100] is quite simple. The carbon hyperfine splittings of the high-field lines are indicated in Fig. 4 and the low-field lines have identical splittings. All the lines of the 20.9-Oe nitrogen hfs triplet have a carbon hfs of 83.1 Oe, while all the lines for which the nitrogen hfs is zero have a carbon hfs of 71.5 Oe.

The initial stages of the analysis of the carbon hfs is best carried out in a coordinate system composed of the three <100> crystal axes. One of these axes, which we call \vec{j}_z , is identical with \vec{j}_1 , the symmetry axis of $\vec{A}^{(N)}$. The other two <100> axes will be denoted as \vec{j}_x and \vec{j}_y . This axis system also is shown in Fig. 3. Since the molecular plane of the HCN⁻ molecule bisects the angle between \vec{j}_2 and \vec{j}_3 , compare Fig. 3, we have from symmetry the simplifying relations

$$A_{xx}^{(C)} = A_{yy}^{(C)}; \quad A_{xz}^{(C)} = A_{yz}^{(C)}. \quad (2)$$

The analysis of the carbon hfs to determine $\vec{A}^{(C)}$ is somewhat more complicated than the procedure used to determine $\vec{A}^{(H)}$ and \vec{g} , because $\vec{A}^{(C)}$ is much more anisotropic than $\vec{A}^{(H)}$ and \vec{g} . Since the g -factor tensor is only slightly anisotropic we may assume that the electron spin is quantized along the external magnetic field. Then Eq. (1) shows that the carbon hyperfine splitting is given by the expression

$$H_{\text{hfs}}^{(C)} = [\vec{A}^{(C)} \cdot \vec{\tau}_H]^2, \quad (3)$$

where $\vec{\tau}_H$ is a unit vector in the direction of the external field. Equation (3) gives the following relations between the carbon hfs observed in the H||<100> spectrum and the components of $\vec{A}^{(C)}$:

$$[A_{zz}^{(C)}]^2 + 2(A_{xz}^{(C)})^2 = 83.1, \quad (4)$$

$$[A_{xx}^{(C)}]^2 + (A_{xz}^{(C)})^2 + (A_{xy}^{(C)})^2 = 71.5, \quad (5)$$

where we have used the relations in Eq. (2).

The spectrum for H||[110], Fig. 5, is the most complicated of the series since it has the largest number of lines and there is considerable overlap among these lines. Fortunately, however, there are enough distinct lines to complete our determination of the components of $\vec{A}^{(C)}$. Consider, for example, the line denoted by B in Fig. 5. Reference to Fig. 2 shows that this is the low-field line of the 14.8-Oe nitrogen hfs triplet in H¹²CN⁻. The low-field lines resulting from the carbon hyperfine splitting of this line are denoted by B' and B'' in Fig. 5, which assignment was verified by considering spectra for angles intermediate between H||[100] and H||[110]. These lines correspond to carbon hfs of 85.3 and 69.1 Oe, respectively, and these splittings are related to

the components of $\vec{A}^{(C)}$ by the equations

$$\left\{ \frac{1}{2} [A_{zz}^{(C)} \pm A_{xz}^{(C)}]^2 + \frac{1}{2} [A_{xx}^{(C)} \pm A_{xy}^{(C)}]^2 + \frac{1}{2} [A_{xz}^{(C)} \pm A_{xy}^{(C)}]^2 \right\}^{\frac{1}{2}} = 85.3, 69.1, \quad (6)$$

where we have again used the equalities in Eq. (2). One cannot tell from the experimental results whether the plus sign in this pair of equations is associated with the 85.3, or the 69.1-Oe splitting. This does not hinder the solution of these equations to obtain the components of $\vec{A}^{(C)}$ but does make it impossible to determine the sign of $A_{xz}^{(C)}$.

Although Eqs. (4-6) give us four equations in four unknowns, these equations are so insensitive to the value of $A_{xy}^{(C)}$ that they cannot give a reliable result for this quantity. To determine $A_{xy}^{(C)}$ we need the carbon hyperfine splitting along one of the <110> crystal axes perpendicular to the symmetry axis of $\vec{A}^{(N)}$. Consider the line denoted as D_2 in Fig. 5. Referring back to the spectrum of H¹²CN⁻ for H||[110], Fig. 2, and the analysis of this spectrum we see that this line is the high-field member of the doublet for which $A^{(N)} = 0$, the doublet splitting being due to anisotropies in \vec{g} and $\vec{A}^{(H)}$. This doublet, together with the central line of the low-field triplet in Fig. 2, was used to determine g_2 , g_3 , $A_2^{(H)}$, and $A_3^{(H)}$. Moreover, since D_2 is the high-field member of the doublet, it is associated with the smaller of these components of g , namely, $g_2 = 2.0005$, and theory has shown that this is the component of \vec{g} along the CN bond.⁶ One of the lines resulting from the carbon hyperfine splitting of D_2 is denoted as D_2' in Fig. 5, this assignment having been made on the basis of similarities in the shape of the lines in the vicinity of D_2 and D_2' . This assignment gives a value of 74.1 Oe for the carbon hfs along the CN bond, which quantity is related to the components of $\vec{A}^{(C)}$ by the equation

$$\{ [A_{xx}^{(C)} + A_{xy}^{(C)}]^2 + 2(A_{xz}^{(C)})^2 \}^{\frac{1}{2}} = 74.1. \quad (7)$$

Equations (4-7) are readily solved by iteration starting with a solution obtained by neglecting all off-diagonal components of $\vec{A}^{(C)}$ in Eqs. (4) and (5) and by neglecting $A_{xy}^{(C)}$ in Eq. (6). The results are:

$$A_{zz}^{(C)} = 82.4, \quad A_{xx}^{(C)} = A_{yy}^{(C)} = 71.0, \\ A_{xz}^{(C)} = A_{yz}^{(C)} = \pm 8.0, \quad A_{xy}^{(C)} = 2.2 \text{ Oe.}$$

In determining the signs it was assumed that all the diagonal components of $\vec{A}^{(C)}$ were positive. These quantities must have the same sign if they are to be consistent with the value found for the isotropic-carbon hfs constant (74.5 Oe).¹ We take the sign to be positive following results obtained for the radicals HCO and FCO.⁷ Diagonalizing the tensor $\vec{A}^{(C)}$ gives the results listed in Table II. The principal axes of $\vec{A}^{(C)}$ are denoted as \vec{j}_1 , \vec{j}_2 , and \vec{j}_3 where \vec{j}_3 is the axis

TABLE II. Principal components (in Oe) of the carbon hyperfine splitting tensor of HCN^- .

$A_1^{(C)} = 90.0$	$A_2^{(C)} = 65.6$	$A_3^{(C)} = 68.6$
--------------------	--------------------	--------------------

perpendicular to the molecular plane. Axis j_1 , makes a 34° angle with \vec{j}_1 . It could not, however, be determined whether \vec{j}_1 is inclined toward the nitrogen atom or away from it. To do this we would need the sign of the quantities $A_{xz}^{(C)}$, and $A_{yz}^{(C)}$ which these experiments did not provide. Since, however, j_1 is the symmetry axis for the approximately axially symmetric tensor $\bar{A}^{(C)}$ it is certain that \vec{j}_1 is oriented so that it approximately bisects the HCN bond angle since this is the orientation of the carbon sp hybrid orbital occupied by the unpaired electron.⁸

Structure of HCN^-

The results for the hfs constants can be used to determine the HCN bond angle (θ) and the unpaired electron charge distribution. This latter quantity is characterized by the unpaired electron charge densities in the following atomic orbitals: (1) the hydrogen $1s$ orbital; (2) a carbon sp hybrid orbital directed along the bisector of the HCN^- bond angle⁸; (3) the in-plane nitrogen $2p$ orbital directed perpendicular to the CN bond. The unpaired electron densities in these orbitals are denoted as ρ_H , ρ_C , and ρ_N , respectively. The process of determining the bond angle and unpaired electron densities from the hfs constants has been described previously for the HCO radical.⁷ The same procedure is applicable to HCN^- except that here we can determine ρ_N directly from the anisotropic part of the nitrogen hyperfine interaction.⁵ The results, together with the previously determined results for HCO, are given in Table III.

The results for the unpaired electron charge distribution in HCN^- and HCO are in agreement with a simple qualitative theory which relates the unpaired electron density on atoms A and B of the radical $H-A=B$ to the electronegativity difference between A and B . If we neglect the hydrogen atom, the unpaired electron in such molecules occupies an antibonding σ molecular orbital (MO) of the form

$$\phi_e = (1 + \lambda^2)^{-1/2} (-\lambda \phi_A + \phi_B). \quad (8)$$

The corresponding bonding MO, which contains two electrons is

$$\phi_b = (1 + \lambda^2)^{-1/2} (\phi_A + \lambda \phi_B). \quad (9)$$

As B becomes more electronegative, the electron charge distribution in the bonding MO becomes concentrated on atom B , i. e., λ increases. Equations (8) and (9) show, however, that an increase in λ , while producing an increase in the total electron charge density on B , reduces the unpaired electron charge density on B . Thus upon replacing the nitrogen atom in HCN^- by the more electronegative oxygen atom to form HCO, there is a decrease in the unpaired electron density on the end atom and a corresponding increase in ρ_C .

The unpaired electron density on the hydrogen atom is the same in HCN^- and HCO despite the differences in bond angle and ρ_C among these radicals. The theory of the proton hfs in radicals of this type predicts that both the increase in bond angle and decrease in ρ_C encountered upon going from HCO to HCN^- should tend to decrease ρ_H .^{6,9} However, this theory also predicts that ρ_H will be very sensitive to the CH bond strength, so that these factors which tend to decrease ρ_H can easily be overcome if the CH bond in HCN^- is somewhat weaker than it is in HCO. (An upper limit of 1.71 eV has been given for the CH bond strength in HCO.¹⁰) A very weak CH bond in HCN^- is consistent with the fact that HCN^- in KCl decays rapidly at room temperature, due presumably to dissociation of the CH bond.² From the activation energy for this reaction, Weatherley estimates the CH bond energy to be 0.95 eV.²

The observed change in bond angle upon going from HCO to HCN^- is in agreement with a somewhat speculative application of Walsh's rules for the shape of $H-A=B$ type molecules.¹¹ These rules are based on a qualitative picture of how the energies of the various molecular orbitals of such molecules change with bond angle, the most significant features of these changes being as follows: (1) As θ varies from 180° (linear molecule) to 90° , the bonding MO's increase in energy and, except for a high-energy antibonding MO which is unoccupied in the ground states of HCN^- and HCO, the antibonding MO's decrease in energy. (2) The changes in the energies of the MO's which accompany molecular bending are due chiefly to the changes produced in the orbitals of atom A . In HCN^- and HCO, only one antibonding orbital is occupied in the ground state. However, a key point of Walsh's argument is that the decrease in the energy of this orbital with molecular bending is so great that it outweighs the corresponding increases in the energies of all the doubly occupied bonding orbitals. Consequently, HCN^- and HCO are bent while HCN is linear. If this picture is correct, then the molecular bending should increase as B becomes more electronegative relative to A because such a change in electronegativity will increase the contribution of orbitals of B to the bonding MO's and, correspondingly, increase the contribution of orbitals of A to the antibonding MO's [compare Eqs. (8) and (9)]. This will make the bonding MO's, which favor a linear configuration, less sensitive to changes in bond angle while the energy of the antibonding MO will decrease faster as the molecule is bent. Thus we may ex-

TABLE III. Bond angles and unpaired electron charge distribution in the HCN^- and HCO radicals.

	HCN^-	HCO
θ (deg)	131	125
ρ_H	0.27	0.27
ρ_C	0.32	0.45
ρ_N	0.41	...
ρ_O	...	0.28

TABLE IV. Components of the electronic g -factor tensors and anisotropic proton hyperfine splitting tensors of HCN⁻ and HCO. All results given in the axis system ($\vec{j}_1, \vec{j}_2, \vec{j}_3$) cf. Fig. 3. Values of components of $\vec{B}^{(H)}$ are in oersteds.

\vec{j}	HCN ⁻	HCO
g_1	2.0023	2.0027
g_2	2.0005	1.9960
g_3	2.0035	2.0041
$B_1^{(H)}$	0.1	-0.8
$B_2^{(H)}$	4.9	5.0
$B_3^{(H)}$	-5.1	-4.2
$B_{12}^{(H)}$	•••	± 5.8

pect that HCO will be more sharply bent than HCN⁻.

Table IV gives the components of the electronic g -factor tensor and the components of the anisotropic part of the proton hfs tensor $\vec{B}^{(H)}$ for HCN⁻ and HCO. The marked similarities between these

quantities further emphasize the similarities between these molecules. These results were also useful in our earlier assignment of the axes $\vec{j}_1, \vec{j}_2,$ and \vec{j}_3 to specific directions in the HCN⁻ molecule. The presence of a measurable off-diagonal component of $\vec{B}^{(H)}$ for HCO established axes \vec{j}_1 and \vec{j}_2 as the in-plane axes for this molecule,⁶ and the similarities between \vec{g} and $\vec{B}^{(H)}$ indicated that these were also the in-plane axes of HCN⁻.

We had begun to study the HCN⁻ ESR spectrum at temperatures intermediate between 4°K where the molecule is rigidly fixed in the KCl crystal and 77°K where it is rotating freely when we became aware of a similar study by Othmer and Silsbee.¹² They find that around 30°K, the ESR spectrum is characteristic of a magnetic Hamiltonian which is symmetric with respect to a [111] crystal axis, and they attribute this to re-orientation of the CN bond among the three equivalent $\langle 110 \rangle$ axes which leave the hydrogen atom in roughly the same position. Our preliminary results are consistent with this interpretation.

*Work supported by U. S. Department of the Navy, Bureau of Naval Weapons under Contract NOW 62-0604-c.

†Present address: The Wellcome Research Laboratories, Beckenham, Kent, England.

¹K. D. J. Root, M. C. R. Symons, and B. C. Weatherley, *Mol. Phys.* **11**, 161 (1966).

²B.C. Weatherley, Ph. D. thesis, King's College, University of London, 1966 (unpublished).

³A. Hausmann, *Z. Physik* **192**, 313 (1966).

⁴A preliminary account of this work was presented at the March 1968 meeting of the American Physical Society in Berkeley, California, E. L. Cochran, B. C. Weatherley, V. A. Bowers, and F. J. Adrian, *Bull. Am. Phys. Soc.* **13**, 347 (1968).

⁵J. R. Morton, *Chem. Rev.* **64**, 453 (1964).

⁶F. J. Adrian, E. L. Cochran, and V. A. Bowers, *J. Chem. Phys.* **36**, 1661 (1962).

⁷E. L. Cochran, F. J. Adrian, and V. A. Bowers, *J. Chem. Phys.* **44**, 4626 (1966).

⁸This orbital, which is denoted as $\phi_{C,e}$, is constructed as a function of the HCN bond angle (θ) by forming three sp hybrid orbitals from the carbon $2s$ and inplane $2p$ orbitals subject to the assumption that the CN and CH σ bonds are formed by equivalent carbon sp hybrid orbitals. Since it will be found from the observed carbon hfs constants that $\theta = 131^\circ$, $\phi_{C,e}$ makes an angle of 24.5° with axis \vec{j}_1 , compare Fig. 3. In the absence of other

contributions to $\vec{A}^{(C)}$, the symmetry axis of $\vec{A}^{(C)}$ will be directed along $\phi_{C,e}$, whereas the observed result is that the approximate symmetry axis of $\vec{A}^{(C)}$ makes an angle of 34° with \vec{j}_1 . The following factors could contribute to this discrepancy: Errors in the measurement of the ¹³C hfs lines, which may be of the order of ± 0.5 Oe; the HCN⁻ radical could be tilted by as much as 5° away from having the CN bond along a [110] crystal axis before the tilt would have a noticeable effect on the nitrogen hfs; invalidity of the assumption that the CH and CN bonds are formed by equivalent carbon sp hybrid orbitals; and contributions to the carbon hfs from spin density in the other in-plane carbon orbitals. We cannot say from the available data how much these various effects contribute. However, it is unlikely that any one of them can account for the entire discrepancy, and it is likely that tilting of the molecule is partly responsible. Also, it can be said that these effects do not change appreciably the results for the HCN bond angle or ρ_C .

⁹E. L. Cochran, F. J. Adrian, and V. A. Bowers, *J. Chem. Phys.* **40**, 213 (1964).

¹⁰G. Herzberg and D. A. Ramsay, *Proc. Roy. Soc. (London)* **A233**, 34 (1955); D. A. Ramsay, *Advances in Spectroscopy*, edited by H. W. Thompson (Interscience Publishers, Inc., New York, 1959), Vol. 1, p. 1.

¹¹A. D. Walsh, *J. Chem. Soc.* **1953**, 2288.

¹²S. Othmer and R. H. Silsbee, *Bull. Am. Phys. Soc.* **13**, 661 (1968).